Three-dimensional, Broadband Seismometer Array Experiment at the Homestake Mine

V. Mandic[a], V.C. Tsai[b], G. L. Pavlis[c], T. Prestegard[a], D.C. Bowden[b], P. Meyers[a], R. Caton[c]

[a] School of Physics and Astronomy, University of Minnesota, Minneapolis, MN 55455, USA
[b] Seismological Laboratory, California Institute of Technology
[c] Indiana University

Introduction

Seismology has been a ubiquitous tool for determining subsurface Earth structure and learning about various dynamic sources, including earthquakes and nuclear explosions [standard seismology REFLay and Wallace 1995; Stein and Wysession 2003]. The number of seismic arrays has grown appreciably in the last few decades, with over 7,000 broadband seismometers deployed within the United States alone, and over 20,000 worldwide [iris REFIRIS 2015]. However, despite this large number of seismometers, instruments have largely been confined to the Earth's surface, with few stations having been placed at depths greater than 100 meters. This is largely a cost issue, primarily due to the obvious practical difficulty of getting to such depths. It has been known since the 1950s (Levin, classic paper in Geophysics) that high frequency noise is dramatically lower when sensors are placed boreholes. For this reason high frequency arrays used in nuclear explosion monitoring have been emplaced in 100 m scale depth boreholes since the earliest work on phased arrays in the 1960s (reference to IEEE papers form 1960s I can easily supply). The few exceptions where deeper boreholes were used have been limited to isolated boreholes (e.g. Abercrombie, 1995)include , the Parkfield borehole seismometer arrays within single boreholes (e.g. Abercrombie 1995; Nadeau and McEvilly 1997; TCDPMa et al. 2012, Parkfield REF). and in active mines (Gibowicz et al. 1991; S. AfricaRichardson and Jordan 2002 and other REF). All of these, however, utilized only , and frequently such instruments have been limited to high frequency geophones ratherhigh frequency sensors. This paper describes the first deployment ever of a phased array with sensors deployed to some of the deepest feasible depths. than more broadband seismometers [REFRichardson and Jordan 2002].

While observing ground motions at or near the Earth's surface has generally been acceptable, there are a number of reasons why observations at deeper depths, particularly from an array of instruments, would potentially be useful. First and foremost, itIt is now well-known that most seismic 'noise' is generated near the surface [noise REF] and that this noise generally decreases significantly with depth [borehole REFMcNamara and Buland 2004]. Observations at depth therefore have the potential to be less contaminated by surficial noisehave higher signal-to-noise ratios, and therefore may more accurately measure the elastic waves arriving from geophysical sources of interestany source. The second main reason that seismic measurements at depth could be advantageous is that

~~Earth structure generally decreases in complexity with depth, with most of the highly weathered and sedimentary deposits being confined near the surface~~the most heterogeneous material we know on the planet is the surface weathered layer [e.g. ~~REF~~Boore and Joyner 1997]. The weathered layer universally has ~~Not only do such features typically cause much~~ slower seismic velocities, and in most cases is wildly variable on a range of scales due to natural variations in weathering process. ~~but they cause the Earth to be highly heterogeneous and~~This makes the near surface nearly always a strongly scattering~~, resulting in complexity of wave propagation that is challenging to model and interpret~~ medium. Since nearly all observations contain this complexity, it is not known precisely how severe the effect is, but it is expected that observations far away from such heterogeneities are simpler and more predictable. Data from the experiment described here has potential for improved insights on the near surface scattering problem.

In addition to illuminating fundamental questions on seismic wave propagation, seismic measurements at depth are also of interest in the field of gravitational wave astrophysics. The Laser Interferometer Gravitational-wave Observatory (LIGO) recently announced the first direct detections of gravitational waves produced in a merger of binary black hole systems (Abbott 2016a, Abbott 2016b), hence ushering a new field of inquiry in astrophysics. To fully explore the scientific potential of this field, more sensitive detectors are being designed such as the Einstein Telescope (Punturo 2010) and the Cosmic Explorer (Abbott 2017). One of the limiting noise factors in these detectors at frequencies below 10 Hz is the seismic noise that causes fluctuations in the local gravitational field. It is expected that this noise source will be reduced underground due to the suppression of seismic surface waves, but it is currently not understood what a sufficient depth for these detectors is, nor what their optimal configuration is. Underground seismic measurements are therefore needed to quantify these effects, thereby directly informing the design of future generations of gravitational wave detectors.

To explore the promise of subsurface seismological observations, both for geophysical and astrophysical applications, we ~~have~~ built and operated an underground three-dimensional (3D) array at the Homestake Mine in Lead, SD. Homestake~~, which~~ was one of the largest and deepest gold mines in North America~~, we report on this unique 3D array in this publication~~. The Homestake Mine officially closed operations in 2002, but reopened in 2007 as the Sanford Underground Research Facility (SURF), and currently ~~features~~ supports several other experiments, including dark matter and neutrino experiments that benefit from the cosmic ray shielding of the rock overburden. The significant infrastructure in the Homestake Mine, including easy access to numerous underground levels with hundreds of km of available drifts, availability of power and digital network infrastructure, and safety protocols and the SURF infrastructure ma~~deke~~ the Homestake Mine an ideal location for the development of a 3D seismometer array.

In this paper, we describe the novelty of the 3D Homestake array as compared to other subsurface seismological deployments, the experience learned in operating the underground array for 2 years, and preliminary results that demonstrate the potential ~~that such data have~~of these data for additional research in the future. ~~While the results~~

~~described here are not expected to be the final products of the Homestake array, we anticipate the results to be useful both for future experiments of a similar type and as a foundation for later analysis.~~

Seismometer Array

The Homestake seismometer array consisted of 24 seismic stations, -15 stations were located underground and 9 on the surface (, depicted in Figure 1). The locations of stations are known with uncertainties on the order of 1 m because of the necessity of precise survey for mining operations and the availability of precision digital maps assembled by SURF. Underground station locations were obtained from ~~maps of the mine drifts based on past mine surveys, while~~these maps. Ssurface station coordinates come from long term averages of GPS data. All of the underground stations were installed between December 2014 and March 2015, and remained operational until December 2016. The surface stations were installed in May 2015 and remained operational until September 2016. The seismic equipment used in the experiment was provided by the Portable Array Seismic Studies of the Continental Lithosphere (PASSCAL) instrument center, which is a part of the Incorporated Research Institutions for Seismology (IRIS). Most stations used a Streckheisen STS-2 high-sensitivity broadband seismometer. The exceptions were the underground station 300 and three surface stations, where we deployed the more water resistant Guralp CMG-3T seismometers.

> **Commented [PMM6]:** The Homestake seismometer array, depicted in Figure 1, consisted of ....

> **Commented [PMM7]:** The exceptions were the underground station on the 300ft level and three of the surface stations, ...
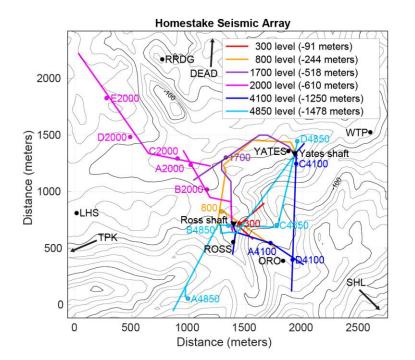
Homestake Seismic Array

Figure 1: Homestake seismometer array layout. The lines of different colors depict the relevant drifts at various depths, along which we installed underground seismic stations. The black filled circles denote the surface stations (remote surface stations DEAD, SHL, and TPK were located outside the depicted region). Also shown are the two shafts at the Homestake mine, known as the Yates and Ross shafts, denoted by black filled triangles.

The underground stations were scattered across several levels: one at a depth of 300ft (91 m), one at 800 ft (244 m), one at 1700 ft (518 m), five at 2000 ft (610 m), three at 4100 ft (1250 m), and four at 4850 ft (1478 m). The locations of these stations were chosen to maximize the horizontal aperture of the array within the constraints imposed by safe access, availability of power, and access to SURF's fiber optic network. In several cases we had to extend existing power and network cables to support the stations. We strove to locate sites as far as possible from activity in the mine and from water drainage pathways. Stations were usually placed in alcoves or blind alleys to minimize the effects of the air drifts, although several stations were installed in enlarged areas within the main drifts of the mine. In most cases, we found there were complex tradeoffs between cost of installation and distance from active operations.

Many sites had existing concrete pads of various sizes and thicknesses from the original mine operation. When necessary we poured a concrete pad directly onto the rock. In all cases a granite tile was attached to the pad using thinset mortar. All underground site

Commented [VCT8]: Tanner commented that Figs1-3 should be vectorized. Perhaps this was done already?

Commented [PMM9]: There seems to be a different font for this caption.

I'm not sure about this image has been vectorized. The couple that I made (figures 2 and 3) were NOT originally in a vector format. However, they'd be exceedingly large if I tried to put them in a vector format. I can do it, but our file will likely then be > 100 MB.

preparation was completed three (or more) months prior to the installation of the instruments. Each seismometer was placed directly onto the granite tile, and was oriented to cardinal directions using an Octans gyrocompass from the IRIS-PASSCAL instrument center. To reduce acoustic noise induced by air flow we covered each sensor with two nested huts constructed of 2" thick polyisocyanurate foam panels and sealed with foam sealant. The digitizer was placed several meters away, and included a Q330 data logger, a baler, and network and power supply electronics. Each station was powered by a small 12V battery continuously charged by a simple AC charger. The battery provided approximately a one day power reserve, which proved more than adequate to cover any power outages encountered during the experiment.

In addition to saving the data locally with a baler, we utilized real-time telemetry for all underground sites and six of the nine surface sites. The underground stations were synchronized using a custom-designed GPS optical distribution system. The GPS signal was received by a GPS antenna mounted on the roof of the SURF administration building and piped to a Q330 in the server room of the same building. This "master" Q330 data-logger was used to convert the received high-frequency GPS signal into the separate 1PPS (1 pulse-per-second) and NMEA metadata components that were used as an external timing signal for the underground instruments. The output from the master Q330's EXT GPS port was fed into an electro-optical transceiver to convert the analog voltage output to optical signals. The transceivers were custom-made for this application by Liteway, Inc. (model number GPSX-1001). An optical-fiber network of optical splitters and transceivers was installed underground to distribute this GPS timing signal to all underground stations, while maintaining its signal-to-noise ratio throughout the mine. At each station, a transceiver was used to convert the optical signals back to electrical, which were then sent into the Q330's EXT GPS port. Phase errors logged by the Q330 digitizers suggest the timing precision achieved with this system was of the order of 1 μs. Systematic errors from propagation and electronic delays were negligible.

Five of the nine surface stations were located on SURF property above the underground stations. Another station was located at Lead High School (LHS) in collaboration with the Lead Deadwood Public School District. We deployed the remaining three stations on private land in an outer ring at a nominal radius of 5 km from the array center. We used conventional, portable broadband sensor vaults but carefully separated the wall of the sensor vault from the concrete pad poured at the bottom. This detail is known from early experience in the 1990s at IRIS-PASSCAL to reduce tilt noise from soil motions. All but one of the sites (DEAD) were bedrock sites with a concrete pad poured on weathered metamorphic rocks of variable lithologies. The surface stations were all oriented by conventional compass methods, which means the precision is less than the underground sites oriented with the Octans instrument. We insulated the sensor vault with a layer of foam and burial with as much of a soil cover as possible. We had the common problem of rain washing some cover away that we restored when the instruments were serviced.

While the three outer stations were stand-alone, the remaining six inner stations all used radio telemetry. Of these, the LHS site located near a high school used a point-to-point radio that linked the outdoor site to a Linux computer in a computer laboratory at the

school. The remaining five stations were radio-linked to a master radio on the roof of the SURF administration building where our data logging computer was located. All surface sites except LHS used solar power; LHS used an AC system similar to underground sites but with a larger battery backup. All surface sites used the standard Q330 GPS timing system.

The telemetry system we deployed used a computer running the Antelope software at the SURF administration building to handle real-time communication to all underground sites and five of the nine surface sites.   We ran a separate Linux computer running Antelope at LHS to handle real-time communications with that single site. This approach was necessary to deal with firewall issues at both SURF and the high school. We then set up an orb2orb feed to a University of Minnesota computer that acted as a data concentrator.   The participating institutions and the IRIS-DMC were then able to tap that connection for real-time feeds with a latency of a few tens of seconds. We developed a custom monitoring system to automatically test for a range of conditions and build web-based quality control summaries. We also set up a rotating shift schedule to monitor this diagnostic information on daily basis. This allowed us to quickly identify and diagnose problems. This was a major factor in the exceptionally high data recovery rate of this experiment (near 100% for every site except DEAD, which had power problems in the winter of 2015-2016). Furthermore, the telemetry data have no mass position related issues except for two sensors failures. In addition, this quality control monitoring allowed us to detect and diagnose a subtle problem on station E2000. That station began showing odd tilt transients, which site visits revealed was created by a failure of the thinset grout on the base of one of our granite tiles. This was repaired by pouring a new concrete pad and setting the tile directly on the concrete.

Preliminary Results

The primary novelty of the Homestake Array is that it is a three-dimensional broadband array, approximately spanning a cubic volume that is 1.5 km on each side (and hence a volume of about 3.4 km^3), in a relatively seismically quiet and geologically stable region. This unusual array configuration leads to both unique opportunities and challenges. In this section, we provide preliminary analyses that demonstrate some of these potential prospects (and issues). The first subsection describes the ambient noise levels of the stations in our array; this noise is found to be nearly as low as some of the lowest-noise stations in the world, suggesting some special capabilities of the array which at some periods are exceptional. The second subsection describes seismic events detected with our array that demonstrate the kinds of event data that were collected in this experiment. As e; as expected for an array of such small aperture, waveforms have a very high degree of coherence, but there are subtle differences between stations at depth and those nearer to the surface that suggest more detailed analysis may yield fruitful information regarding near-surface heterogeneity. Finally, since the results presented here represent only a first study ofinitial work on this dataset, in the nextfinal subsection we discuss some of the other directions we envision the Homestake array dataset will be useful forconsiders possible future applications of these data.

<div>
Commented [PMM13]: Should we include a source for the Antelope software?
</div>

<div>
Commented [VCT14]: See next comment
</div>

<div>
Commented [VCT15]: Tanner suggests being more specific. Modern seismic arrays have a wide range of recovery rates, from <50% (e.g. for some remote island stations without power) to better than ours (i.e. 99.99%). Not sure that our recovery is actually "exceptional". Perhaps the reason that it might be exceptional is that it was an unusual environment, rather than a "standard" seismic deployment.
</div>

<div>
Commented [GP16]: Putting on my hat as chair of the IRIS Instrumentation Services committee I can tell you that this is very exceptional. GSN is only abou 90%, and most PASSCAL deployments are low 80-90%. The only operations I know with a better performance are AFTAC gold-platted DOD supported arrays and the Earthscope TA.
</div>

<div>
Commented [VCT17]: I think this section needs a preamble, so I tried to write one. It partly motivates the array again, and introduces what will be discussed. Feel free to modify/add.
</div>

<div>
Commented [GP18]: Being in the stable interior is not such novelty and more of a negative from a seismologists perspective – no local earthquakes
</div>

Noise Spectra

The ambient seismic noise levels at the Homestake mine, especially at the deepest levels, are remarkably low and stable. We demonstrate this by computing the displacement amplitude spectral density (ASD) of seismic noise over long periods, for different stations and for different seismic channels (east, north, vertical). We use one year of data (from June 1, 2015–May 31, 2016), split into 400 second intervals. The median amplitudes in each frequency bin for the vertical seismic channel are shown in Figure 2 in comparison to the low- and high-noise models of Peterson [1993 REF]. The left panel compares the ASDs for stations at several different depths. All of the stations are in close agreement in the middle range of frequencies (0.1-0.5 Hz), which corresponds to the microseismic peak. At higher frequencies, there is significantly less noise with depth: above 0.5 Hz, the stations at 4100 ft and 4850 ft depths are nearly an order of magnitude quieter than other stations. At the lowest frequencies (<0.1 Hz), there is also a good agreement between the stations, although a slight increase in noise is apparent at the surface stations; this may be due to larger temperature variations closer to the surface that induce tilts in the concrete pads. While the underground stations at any given depth tend to agree very well, there is a wide range of variability among the surface stations, as depicted in the right panel of Figure 2. This is due to differences in the local environment in terms of thermal insulation and proximity to human activity.
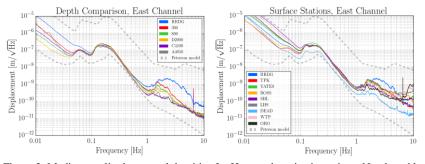

Figure 2: Median amplitude spectral densities for Homestake seismic stations. Numbered legend entries denote depth in feet, while numberless legend entries denote surface stations. Peterson low- and high-noise models are shown as dashed gray lines. See text for more detail.

Figure 3 shows ASD histograms for the RRDG surface station (left-) and for the A4850 underground station (right) as examples of a relatively good surface station and our deepest and most isolated underground station. Here, the histograms of ASDs are calculated from 400-second data intervals over 1 year in each frequency bin, revealing the overall variability of the seismic noise at each station. The white curve represents the median ASD (identical to those shown in Figure 2), the black curves represent the 95% confidence intervals in each frequency bin, and the color scale shows the overall distribution. The Peterson low- and high-noise models are shown in dashed gray.

The histograms display about two orders of magnitude of variation across all frequencies for both the RRDG station and the A4850 station. The A4850 station measures less noise

Commented [PMM19]: These are now made from January 2015 to December 2016 (using all available data). Also, I used 900s intervals instead of 400s intervals.

Commented [VCT20]: Are these vertical component? Fig2 labels it as East.

Commented [VCT21]: Tanner suggests noting these are constructed primarily from surface stations? I would suggest taking a slightly different tack, i.e. re-emphasizing that our stations are at depth.

Commented [VCT22]: If these are horizontal components, that's a reasonable explanation. If vertical, I'm not so sure.

Commented [VCT23]: Why is the Deadwood station so good? It looks to be nearly identical to A4850, or even better. Is the lack of (7s) microseism related to it dying (not recording) in the winter? If so, that would be slightly misleading.

Commented [PMM24R23]: I'm not sure. There are a few possibilities. I'll take a look at the DEAD data and see if maybe there was something I missed.

Commented [PMM25]: Relatively good -> representative

in general and appears to have less overall variation than RRDG. There also appears to be significantly more high-frequency noise in the RRDG station; this is likely due to anthropogenic surface waves that are suppressed with depth. Both stations stay within the low- and high-noise Peterson models most of the time. However, in the 0.3–0.9 Hz range the A4850 station is actually below the low-noise model a significant fraction of the time. We also observe a considerable difference between the vertical channel and the horizontal channels at low frequencies. At: at 0.01 Hz and below for both stations, the vertical channel on both stations haves almost an order of magnitude lower noise than the horizontals, likely caused by the slow tilting of the ground.. This is nearly universal on broadband instruments and is well known to be a result of tilt noise that is increases with period on horizontal components (Weillandt reference – I (glp) need to find it). The horizontal components of the underground sites are exceptionally quite and from very long time series we see tidal signals with very signal-to-noise ratios.(Ross has some amazing recent results on this, but they do not belong in this paper. I recommend a simple sentence like given the objective of this paper.)
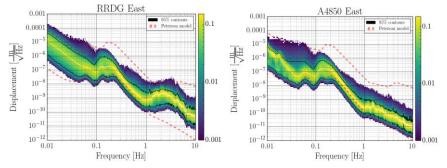

Figure 3: Histograms of amplitude spectral density in each frequency bin for a surface station (left) and for an underground station at 4850 ft depth (right). Median ASDs (solid white), 95% confidence intervals for each frequency bin (solid black), and the Peterson low- and high-noise models (dashed gray) are shown. See text for more details.

The low-noise levels of a significant fraction of our stations at depth suggests that the array may be useful for better understanding how ambient noise levels depend on depth, and in particular what fraction of the noise is spatially and temporally coherent. Such a study, which cannot be done with a single borehole seismic station, is beyond the scope of this contribution, but is expected to be discussed in future contributions.

Array Analysis of Event Data

Detecting and analyzing seismic events in an area with otherwise sparse station coverage using our small-aperture array of 24 ultra-quiet sites was technically challenging since conventional automated detectors typically assume all sites provide equally weighted independent data. Thus, attempts at automatic detection using Antelope 5.6 (BRTT 2017) applied to our array data augmented by data from 8 regional stations (see Fig. 4b) resulted in a large number of spurious detections. We solved this issue, and reduced the

Commented [VCT26]: I think we need a paragraph that discusses implications of these specific results. I tried to make a brief one here, but anyone feel free to add/modify.

Formatted: Font: Not Bold

false detection rate to near zero, by running the detection algorithm only on the three outer surface sites (DEAD, TPK, and SHL), one of the quietest underground sites (D4850) and the 8 regional stations, and by requiring six P-wave associations before declaring an event. These choices resulted in significantly raising the detection threshold, and no longer detecting events from a local active surface mine, located only 2.5 km west of station TPK. A large number of such very local events exist (see Fig. 5 for one example), indicating at least one blast per day during the workweek, and could be used in future studies. For example, Figure 5 clearly shows the theoretically expected suppression of Rayleigh waves with depth, with Rayleigh waves barely visible on any of the stations in the 4000s subarray. However, we will not discuss these events further in this contribution.

Standard analyst review of the revised detection routine applied to six months of data (January-July 2015) resulted in the detections shown in Figure 4. Of the 431 epicenters, 359 are in the local area shown in Fig. 4b and 72 are at regional to teleseismic distances shown in Fig. 4a. The locations shown in Fig. 4a were produced by association of events with those from the U.S. Geological Survey catalog (ANF 2017) and using the associated epicenters. L, whereas locations in Fig. 4b were estimated with the dbgenloc program (Pavlis et al. 2004) assuming the IASPEI91 earth model. All of the 359 local events in Fig. 4b are likely to be coal mining explosions from the Powder River Basin. All have similar waveforms with emergent P waves and prominent surface waves like the event shown in Figure 5. Despite assuming fixed depths (of zero), some epicenters were poorly constrained and likely badly estimated due to too few of the regional stations having detection picksobservable P or S waves. Most well located events cluster in the coal mining district, supporting our hypothesis that these are mining related.

To date we have processed six months of data to identify seismic events. This has required a mix of conventional and unconventional analysis. A technical problem we faced is that this array was located in an area with some of the sparsest coverage in the country. In an area with sparse coverage, an array of 24 ultra-quiet sites dominates detection limits and violates implicit assumptions of conventional automated detectors. Figure 4 shows the 8 regional stations we used to detect and locate local and regional events. We used the automated detectors and location system in Antelope 5.6 (http:://brtt.com latest access April 25, 2017). When we used all channels from the array in combination with the sparse regional coverage we had a large number of spurious detections. Although some of such detections are definitely local sources that might be of interest in other studies, our initial interest was in the events with the best signal-to-noise ratio where the plane wave approximation was valid for phased array processing. We reduced the false detection rate to near zero by running the detection algorithm only on the three outer surface sites (DEAD, TPK, and SHL) and one of the quietest underground sites (D4850), and by requiring six P-wave associations before declaring an event.

The most significant impact of this choice is that we stopped detecting all of the events from a local mine, with example seismograms from such an event shown in Figure 5. The source for those seismograms is without doubt an active surface mine whose

boundary is only 2.5 km west of station TPK.   The detections shown in Figure 4 are thus

Figure 4.   Epicenter maps of events recorded by Homestake 3D array. (a) An azimuthal equal distance projection map centered at the array site marked with a star. Epicenters of distant earthquakes recorded by the array in the 2015 study period are shown as circles. (b) Epicenter map focused on local and regional events. The array location is again shown as a star and estimated event epicenters are shown as circles. Black filled triangles are regional stations used for detection and location of the events plotted.

We used a standard analyst review method to produce the epicenter maps shown in Figure 4. Of 431 epicenters, 359 are in the local area shown in the right panel of Figure 4 and 72 are at regional to teleseismic distances shown in the left panel of Figure 4. The locations shown in Fig. 4a were produced by association with epicenter estimates produced by U.S. Geological Survey catalogs and assembled at the USArray Array Network Facility (http://anf.ucsd.edu/events/ last access April 27, 2017). We estimated the local event epicenters shown in Figure 4b with the dbgenloc program (Pavlis et al., 2004) using the IASP91 earth model and travel time picks made by standard, interactive analyst review methods.   All of the 359 events shown in Figure 4b are likely to be mining explosions from coal mining in the Powder River Basin.   All have similar waveforms with emergent P waves and prominent surface waves like the event shown in Figure 5.   We assumed this was the case and fixed the depth of all these events for the location estimates used for Figure 4b to zero. Most of the events cluster in the area of the coal mining district. There are some outliers that are almost certainly poorly constrained epicenter estimates that have been badly mislocated.   These events are characterized by picks at only one regional station in addition to the array, which creates a poor constellation for location.

Figure 5.   Vertical component seismograms from local surface mine. Seismograms are displayed at true amplitude and grouped by subarrays used throughout this paper. Records for each subarray are sorted by epicentral distance from the estimated source location (approximately 4 km west of TPK).   Subarrays are ordered by increasing depth.

Figures 6 and 7 show three-component subarray stacks for two representative events. Since we found systematic differences in waveforms with sensor depth, these subarray

stacks were grouped into three subarrays defined in Figure 5 ('Surface', '2000s' and '4000s'). Note that we treated the 300 and 800 stations as part of the 'Surface' subarray, grouped the 1700 station with the five 2000-level stations in the 2000s subarray, and grouped the 4100 and 4850 stations in the 4000s subarray. Such systematic differences are expected due to near-surface effects that have been known to complicate seismic array processing since the early VELA UNIFORM experiments of the 1960s (REFERENCES). To produce each subarray stack, we used an array-based cross-correlation algorithm to align signals prior to stacking (Pavlis and Vernon 2010). Typical correlation window lengths were 2-4 s for the local mining blasts and 10-20 s for the teleseismic events. The stacked signals of the 3 subarrays were then manually aligned to produce the figures shown.

~~We processed all the events with locations shown in Figure 4 with a nonstandard array processing method. When we examined waveforms recorded by the array it was clear that simple delay and sum phased array processing was problematic. We found a strong systematic difference in waveforms with sensor depth. We expected this because near surface effects have been known to complicate seismic array processing since the early VELA UNIFORM experiments in the 1960s (REFERENCES). Because of the array geometry, we grouped the array into three subarrays defined in Figure 5. Note we treated the 300 and 800 station as part of the SURFACE subarray and grouped 1700 with the five stations on the 2000 level to define the 2000s subarray. The stations on 4100 and 4850 were grouped as the 4000s subarray. We then utilized a "subarray" option on the dbxcor~~
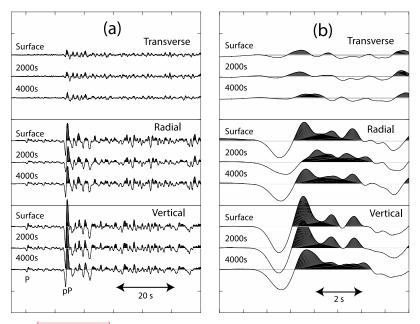
.

Figure 6: Displacement [? Velocity?] seismograms from an Alaskan earthquake recorded by the Homestake 3D array.   (a) illustrates the three components of subarray stacks defined in the text. (a) shows the first 2 minutes of the data following the P wave signal. These data were filtered with a 0.01 to 2 Hz bandpass filter before stacking. The P wave of this event is much smaller than the pP phase seen approximately 25 s after P (event depth is 120 km and distance is 33°). (b) shows a shorter time window focused on only the P wave (6 s following measured P time). All plots are true amplitude meaning amplitudes differences between seismograms are real.   In all figures the seismograms have been aligned by cross correlation before stacking. Stacks are aligned manually.
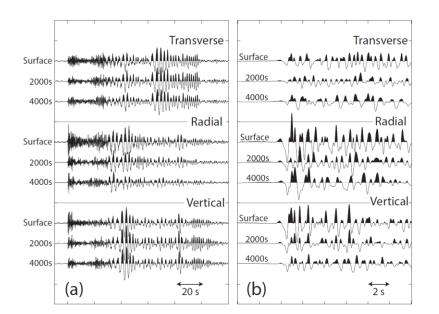
Figure 7: Seismograms from a typical Powder River Basin coal mining explosion recorded by the Homestake 3D array.   All the data shown in this figure were filtered with a 5 pole Butterworth filter with a pass band from 0.25 to 10 Hz. (a) shows 2 minutes of data following P-wave and is directly comparable to Figure 6a. (b) is directly comparable to the Figure 6b but for this explosion source instead of a teleseismic earthquake.   (b) shows subarray stacks for 6 s of data following the measured P wave time. We show the 2000s subarray here because for this event that subarray is oriented roughly in the direction of propagation of the P-wave. All figures show seismograms in true amplitude and seismograms were again aligned by a mix of cross-correlation and manual picks.

~~Figures 6 and 7 show the three components of the stack of the aligned seismograms from each subarray for two representative events.~~ Figure 6 shows subarray stacks from an intermediate depth event in Alaska where the pP phase is significantly bigger than P. Nonetheless, the P signal shown magnified in Figure 6b has a very high signal-to-noise ratio and a relatively high frequency content for a teleseism. Figure 7 shows comparable results for a typical, larger Powder River Basin mining explosion. ~~These figures show why subarray stacks are a necessary approach for handling these data.~~ The subarray stacks show significant differences in waveforms that are unquestionably not related to background noise. Figure 7 shows a secondary amplitude effect not seen in the teleseismic waveforms. ~~Notice the~~In particular, there is a strong change in amplitude with depth, with the average surface-station P wave roughly a factor of 2 higher amplitude that the 4000s subarray average. A comparable difference in P-wave amplitude is not seen for the teleseismic signal in Figure 6.   How much of that

difference is due to the differences in emergence angle (steep angle of incidence for the teleseism but approximately horizontal for the mining explosion) and how much of the difference is due to frequency content (upper limit around 2 Hz for the teleseism and upper limit near the 40 Hz antialiasing frequency corner for the mining explosion) is not yet clear.

These results, though preliminary and exploratory, further ~demonstrate the potential of the Homestake array dataset to be used to explore the role of near-surface structure in complicating in earthquake waveforms. Unlike with surface arrays, where the complexity of near-surface structure is convolved with complexity of earthquake sources, the Homestake array's geometry allows for separate evaluation of these two aspects of earthquake waveform modeling. While some of this separation is possible with single borehole arrays, the linear geometry inherent in such arrays is a clear drawback, leading to significant underdetermination of inversions that the Homestake array data should suffer less from.

Future ~~work~~directions:

As described earlier, we expect the unusual array geometry to be useful for a number of analyses in addition to the two examples provided. Several such studies are already underway, and here we briefly describe some of these possibilities, which will be subjects of future publications.

> **Commented [VCT34]:** More text here as a preamble? Feel free to make suggestions.

In the analysis of ambient noise, the depth extent of the array may be useful in helping estimate the directionality and modal content of the seismic noise. For example, the depth dependence of the observed Rayleigh and Love eigenfunctions can be used as a direct constraint on the modes observed, rather than having to make assumptions about the dominance of fundamental-mode surface waves that are commonly made. Combined with other radiometer-based techniques used in other areas of physics (REFERENCE), such estimates would directly contribute to the design of future underground gravitational-wave detectors.

For teleseismic earthquake analysis, other analyses beyond what was described previously may also help understand the scattering and reflection of the nearly-vertical incoming waves with the surface, hence directly measuring the impact of the surface weathered layer on the teleseismic waveforms. One example that is being pursued relates to how well one station's waveforms can be predicted based on knowledge of all other stations' data. The dependence of station location on the success of such predictions should provide valuable information about the heterogeneity of subsurface structure.

Finally, comparison of P-wave particle motions within the array may yield unique data on P-wave anisotropy. The rocks at Homestake are predominately highly foliated phyllites and schists (REFERENCE) and are known to be highly anisotropic (REFERENCE). It is thus not surprising that most of the events we have examined (e.g., Fig. 6 and 7) show significant amplitudes on the transverse component, even during the first cycle of the P

wave. Further analysis will be necessary to fully identify how strongly anisotropy affects observed waveforms.

Conclusions

We have described a three-dimensional array of high-sensitivity broadband seismometers in the Homestake mine, SD, spanning roughly a cubic mile underground. We have also shown preliminary results of analyses of data acquired by this array. The data are characterized by exceptionally low seismic noise levels that are also very stable over a year-long time scale. Consequently, the data offer a wide range of possible studies to better understand wave propagation. The data contains high signal-to-noise records of hundreds of transient signals, both due to local or regional mining blasts and due to teleseismic events. A preliminary look at these transient events reveals rich structure in terms of depth dependence of different wave components, and in terms of interaction of waves with the surface.

Several studies are underway examining some of these effects in further detail. The transient events offer multiple ways to estimate the seismic wave speed, both locally in the Homestake mine, and in the region. The depth dependence of waveforms in these transients is also used to determine the depth eigenfunctions for Rayleigh and Love waves. This information will be combined with radiometer-based techniques used in other areas of physics to attempt estimates of directionality and modal composition of the ambient seismic noise. Such estimates would directly contribute to the design of future underground gravitational-wave detectors. The depth and temporal dependence of teleseismic events is also being used to understand the scattering and reflection of the nearly-vertical incoming waves with the surface, hence directly measuring the impact of the surface weathered layer on the teleseismic waveforms. Finally, active excitation experiments were conducted, with excitations performed both on the surface and underground, providing additional information on wave propagation, reflections, and scattering. These studies will be subjects of future publications.

> **Commented [VCT36]:** As suggested in the previous section, I think some of this could be described briefly in the previous section. I realize we don't want to nor can we say too much, but perhaps more than this would be possible, or at least motivation for these studies could be provided.

> **Commented [VCT37]:** I stole many sentences from this paragraph to fill the "Future directions" section, so this needs to be rewritten to not be repetitive. In the future directions section, I did not mention estimates of wave speeds or the active excitations, both of which I see as being helpful for us, but not end goals in themselves. Let me know if you have thoughts about how to best mention them, and also about how to modify this ending paragraph.

References

Abbott, B. P. et al. (The LIGO Scientific Collaboration and Virgo Collaboration) (2016a), Observation of Gravitational Waves from a Binary Black Hole Merger, *Physical Review Letters* **116**, 061102.

Abbott, B. P. et al. (The LIGO Scientific Collaboration and Virgo Collaboration) (2016b), GW151226: Observation of gravitational waves from a 22-solar-mass binary black hole coalescence, *Physical Review Letters* **116**, 241103.

Abbott, B. P. et al. (The LIGO Scientific Collaboration and Virgo Collaboration) (2017), Exploring the sensitivity of next generation gravitational wave detectors, *Classical and Quantum Gravity* **34**, 044001.

Abercrombie, R.E. (1995). Earthquake locations using single-station deep borehole recordings: implications for microseismicity on the San Andreas Fault in southern California, *J. Geophys. Res.*, **100**, 24003-24014.

ANF (2017). Array network facility of USArray website, http://anf.ucsd.edu/events/ last access April 27, 2017.

Boore, D.M. and W.B. Joyner (1997). Site amplifications for generic rock sites, *Bull. Seismol. Soc. Am.*, **87**, 327-341.

BRTT (2017). Boulder real time technologies website, http:://brtt.com latest access April 25, 2017.

Gibowicz, S.J., R.P. Young, S. Talebi, and D.J. Rawlence (1991). Source parameters of seismic events at the underground research laboratory in Manitoba Canada: scaling relations for events with moment magnitude smaller than -2, *Bull. Seismol. Soc. Am.*, **81**, 1157-1182.

IRIS (2015). 2015 annual report, http://www.iris.edu/hq/files/publications/annual_reports/doc/2015_iris_annual_report_rev10-29-15.pdf.

Lay, T. and T.C. Wallace (1995). Modern global seismology, Academic press, San Diego.

Ma, K.-F., Y.-Y. Lin, S.-J. Lee, J. Mori, and E.E. Brodsky (2012). Isotropic events observed with a borehole array in the Chelungpu Fault Zone, Taiwan, *Science*, **337**, 459-463.

McNamara, D.E. and R.P. Buland (2004). Ambient noise levels in the continental United States, *Bull. Seismol. Soc. Am.*, **94**, 1517-1527.

Nadeau, R.M. and T.V. McEvilly (1997). Seismological studies at Parkfield V: characteristic microearthquake sequences as fault-zone drilling targets, *Bull. Seismol. Soc. Am.*, **87**, 1463-1472.

Pavlis, G. L. and F. L. Vernon (2010). Array processing of teleseismic body waves with the USArray, *Computers and Geosciences*, **36**(7), pp. 910-920.

Pavlis, G. L., F. L. Vernon, D. Harvey, and D. Quinlan (2004). The generalized earthquake location (GENLOC) package: A modern earthquake location library, *Computers in Geosciences*, **30**, 1079-1091.

Peterson, J. (1993). Observations and modeling of seismic background noise, *USGS Open-File Report*, **93-322**.

> **Commented [VCT38]:** Alternatively, we could just cite www.iris.edu/mda, which may be more relevant anyway

M. Punturo et al. (2010), The third generation of gravitational wave observatories and their science reach, *Classical and Quantum Gravity* **27**, 084007.

Richardson, E. and T. Jordan (2002). Seismicity in deep gold mines of South Africa: implications for tectonic earthquakes, *Bull. Seismol. Soc. Am.*, **92**, 1766-1782.

Stein, S. and M. Wysession (2003). An introduction to seismology, earthquakes, and earth structure, Blackwell publishing, Malden MA.